Journal of Molecular Graphics and Modelling 41 (2013) 89–96

Contents lists available at SciVerse ScienceDirect

Journal of Molecular Graphics and Modelling

journal homepage: www.elsevier.com/locate/JMGM

DFT modeling of CO_2 adsorption on Cu, Zn, Ni, Pd/DOH zeolite

Daniel Smykowski[a,*], Bartłomiej Szyja[b,c], Jerzy Szczygieł[a]

[a] Wrocław University of Technology, Department of Chemistry, Gdańska 7/9, 50-344 Wrocław, Poland
[b] Inorganic Materials Chemistry, Department of Chemical Engineering and Chemistry, Eindhoven University of Technology, Den Dolech 2, 5612AZ Eindhoven, The Netherlands
[c] Institute for Solid State Theory, University of Münster, Wilhelm Klemm Str. 10, Münster, Germany

ARTICLE INFO

Article history:
Accepted 29 January 2013
Available online 16 February 2013

Keywords:
CO_2 adsorption
DFT
Zeolites
Catalyst
Molecular dynamics

ABSTRACT

This study is the analysis of the adsorption process of the CO_2 molecule on the cationic sites of the DOH zeolite. Based on the DFT method, we have been able to identify several adsorption sites containing extra-framework cations and evaluate the value of the adsorption energy with respect to the distance from the adsorption site. The zinc cation has been found to cause the strongest interaction with the CO_2 molecule. Subsequently, the adsorption process has been investigated by means of the Molecular Dynamics simulations. The results of the MD simulations are consistent with the geometry optimizations, and confirm the activation of CO_2 molecule adsorbed in the Zn site.

1. Introduction

Fossil fuels are still the most significant sources of energy and their consumption is dynamically rising. At the moment, there is no real alternative to conventional energy sources, so it is predicted, that consumption of fossil fuels will increase in future [1].

Combustion of these fossil resources consequently leads to the emission of carbon dioxide [2]. Alongside its negative influence on the climate (CO_2 content in the atmosphere has changed from 313 ppm (1960) to 389 ppm (2010) [3]), carbon dioxide is a useless waste. Some part of CO_2 is utilized in natural way (photosynthesis), but at the moment there is no technology for effective conversion of CO_2 into useful and highly demanded products in order to utilize large amounts of CO_2.

Many solutions for carbon dioxide utilization have been proposed [4], including underground and underwater storage (known as "carbon sequestration" or "carbon capture") [4], CO_2 reforming of methane [5], electrochemical reduction of carbon dioxide [6,7], conversion to carbon monoxide and methanol, production of dimethyl ether [8,9]. Extensive review of methods for carbon dioxide utilization was presented by Wang et al. [10]

Apart from carbon capture, the interesting concept is hydrogenation of carbon dioxide into hydrocarbons, which could be used as fuel components [11–13], similarly (also from the thermodynamic aspect) to the Fischer–Tropsch synthesis [14]. Fuel-like hydrocarbons are highly demanded products, so conversion of carbon dioxide into hydrocarbons might be, in opposite to other mentioned methods, a solution to utilize large amounts of CO_2. Another advantage of such a conversion is production of fuels without making use of fossil resources.

Reduction of carbon dioxide requires a proper catalyst in the same extent as carbon capture requires proper adsorbent. A large variety of catalysts has been already studied, including metal oxides like TiO_2 (anatase) [15], polyoxometalates [16], rhodium complexes [17], iron–manganese catalyst [18], iron and cobalt catalysts [13], ceria [19], iridium complexes [20], mesoporous silica supported Cu/TiO_2 catalysts [12] or zeolites [21–23]. Yamashita and Anpo found that metal containing zeolites (including transition metals) may be good candidates for CO_2 reduction catalysts [21–23]. Additionally, catalyst surface plays significant role in activating CO_2, possibly by decreasing the O—C—O bond angle, as reported by Indrakanti et al. [15], for which the presence of oxygen defects in TiO_2 (anatase) catalyst surface has been found to be essential. It was also reported, that reduction due to the direct electron transfer between defect-free anatase surface and CO_2 is unlikely.

Both processes described above, share the adsorption as a common event. Adsorption of substrates is the key step of every process carried over heterogeneous catalyst, so detailed analysis of this phenomenon is necessary to design a catalyst. In this paper, the aim of the study was to investigate the dependence between the extra-framework cations in zeolite structure and its adsorption properties with respect to the carbon dioxide molecule.

2. Computational details

The scope of the study is the adsorption of a single molecule and calculation of adsorption energy for both unmodified DOH

* Corresponding author. Tel.: +48 71 320 64 06.
E-mail address: daniel.smykowski@pwr.wroc.pl (D. Smykowski).

1093-3263/$ – see front matter © 2013 Elsevier Inc. All rights reserved.
http://dx.doi.org/10.1016/j.jmgm.2013.01.009

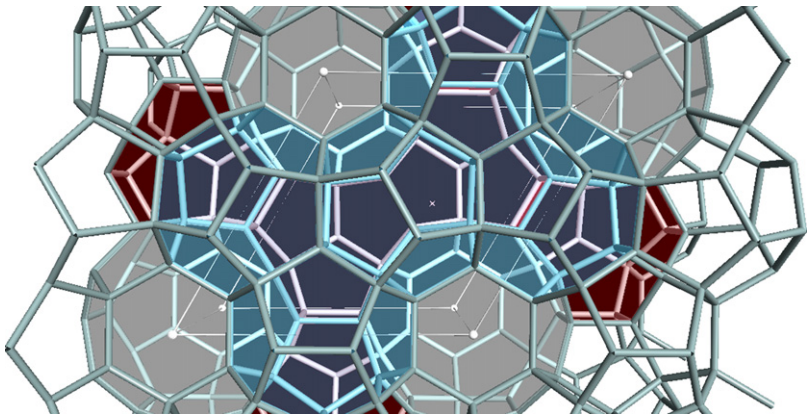

Fig. 1. DOH zeolite structure framework. Three different tiles are marked with colors: gray denotes t-doh, blue t-red and red t-doo. White wire-frame shows the boundaries of the unit cell.

structure and structures modified with extra-framework cations. This part of the work allowed to point out the adsorption centers. Subsequently, the molecular dynamics simulations were performed in order to study behavior of the host–guest systems in time, and to investigate the configuration of the CO_2 molecule near the adsorption center.

The computational procedure used in this work can be divided into three parts. Construction of models having different substitution sites (a), evaluation of the host–guest interactions with the molecule adsorbed in the arbitrary locations (b) and insight into adsorption process (c).

2.1. Construction of models

The selection of the ideally suited framework cannot be done with the DFT method due to the overwhelming amount of the framework/cation combinations possible. The extensive study on the suitability of different zeolite framework has been done in the group of B. Smit [24]. In our study we decided to choose DOH zeolite.

The structure was imported from Accelrys Materials Studio structure library [25]. The DOH framework was chosen due to its characteristic structure. Whereas the DOH structure might not be the best candidate for the carbon capture, it contains 4-, 5- and 6-membered silicate rings, as well as the cages (tiles) of different size interconnected with the different rings. This structure gives the opportunity to perform the most systematic study possible on only one structure.

DOH framework has zero-dimensional channel system, it has however three types of tiles that consist to the framework. According to Database of Zeolite Structures [26] the largest one is named t-doh (shown in gray in Fig. 1), and consists of eight 6rings and twelve 5rings. It interconnects with next t-doh tile by the top and bottom 6ring. There is only one t-doh tile per unit cell, it is located along the cedge of the unit cell. Side 6ring connects t-doh tiles with t-doo tiles which are the smallest ones (shown in red in Fig. 1), and contain also three 4rings and six 5rings. There are 2 t-doo tiles per unit cell, they interconnect by the 4rings to each other. Both t-doh and t-doo tiles connect with the t-red tile (shown in blue in Fig. 1) by the 5rings. The t-red tile contains only twelve 5rings in the structure. There are 3 t-red tiles per unit cell.

As there are literature sources citing the necessity of two types of catalytic sites in reduction reactions, one being metal cations other strong acids [27], we have modified DOH zeolite structure by exchanging selected Si atoms to Al atoms [28,29] and negative charge was compensated either by +2 cations: copper, zinc, palladium or nickel. In this way substitution of two Si atoms with Al atoms allows to introduce one bivalent cation.

Substitution places were selected according to the Löwenstein's rule. Because the aim was to introduce +2 cations (Cu, Ni, Zn, Pd) in specific locations, it was necessary to exchange two Si atoms possibly close to each other. Some of the models used in first part of the study contain more than one cation.

In order to study many different cation sites, we have introduced Si → Al substitutions in all silicate rings present in the unit cell. In our work we decided for the following nomenclature: the 6ring substitution in the 6ring connecting two t-doh tiles is named 6rb (as in connection between two "big" tiles), and in the 6ring connecting t-doh and t-doo is named 6rs (as in connection with "small" tile). Analogously 5rings that can connect tred with tdoh are named 5rb, as t-doh tile is bigger than t-red, and t-red with t-doo are named 5rs, as t-doo is smaller than t-red. The 4rings can only connect small t-doo tiles, therefore they are named 4rs.

Substitution places for models used in this work are presented in Fig. 2. The substitution in the different ring structures lead to differences in the location of counter cations compensating the charge. The 6-ring is the biggest one present in the structure, and the cation fits in the plane of the ring, however smaller 5rings can cause the cation to lift up from the inplane position. The direction in which the position of cation is shifted from the 5rs position leads to the symmetrically equivalent positions of cation in either of the t-red cages that 5rs connects. The 5rb substitution however, can lead either to shifting the cation toward big t-doh or small t-doo cages.

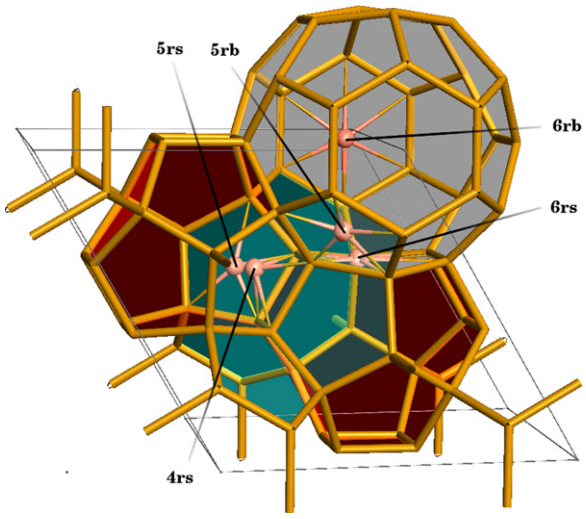

Fig. 2. Substitution places in investigated models shown schematically in one structure.

We have decided to move the cation toward the larger t-doh cage, as there was already a model built that contains a cation in smaller t-doo cage. This effect however is relatively small even for large Pd cation.

As far as 4ring is concerned, the shift from the inplane position is much bigger, but as 4ring connects identical tiles, the direction where the cation is shifted from the ring again leads to symmetrically equivalent positions.

In this work we have decided on two approaches of studying the location of the CO_2 adsorption site with respect to the cation substitution. First option was to use only one adsorption site, and introduce the cation in different locations in the framework, whereas the second was to keep one substitution present, and adsorb the CO_2 molecule in different adsorption centers.

2.2. Location of potential adsorption sites

There are many computational algorithms which purpose is to find the location of potential adsorption centers inside porous solids. One of the possible approaches is making use of available codes designed for this purpose. We have decided however to implement our own algorithm that fulfilled our needs. The reason behind this was to enable as many potential adsorption sites as possible, even not optimal ones that represent most stable configurations. Studying these sites allows us to investigate the effect of the distance of the CO_2 adsorption site from the substitution place. We have therefore implemented another scheme of finding the possible adsorption sites—a plug-in named Docking Tool has been developed for Zeobuilder program [30]. The aim of the Docking Tool was to generate random positions of the adsorbate (in this case CO_2 molecule) in the zeolite structure and create input files for subsequent optimization in SIESTA [31,32]. Algorithm for generating random configurations is presented in the form of block scheme in Fig. 3.

Ideally, the CO_2 molecules should be placed in a local or a global minimum on the potential energy surface, or as close to the minimum as possible. This can be achieved in two ways—one requires the evaluation of the energy of the system for each configuration, similarly to the GCMC method [33]. However, that would be very time consuming, as most of the randomly chosen configurations would overlap the atoms of CO_2 with the atoms of the zeolite framework. We have therefore decided to implement another solution.

To determine the optimal atom–atom distance we have determined the energy vs. distance dependence of the CO_2 molecule and the active center. The first step was to build zeolite cluster with CO_2 molecule. The cluster was cut from optimized structure of DOH_4RS_1Zn with carbon dioxide molecule. Terminating hydrogens were located in place of Si atoms in original structure. Distance O–H was set to 0.966 Å [34]. The single-point energy of this system was calculated, then CO_2–cation distance was changed, in order to scan the CO_2–cation distance and calculate the energy. This is shown in Fig. 4.

Basing on the above, we have "translated" the energetic criterion to the geometric one, with the closest atom–atom distance in docking simulations was set to 1.7 Å. Although the algorithm itself does not check the energy of the system for different location of the guest molecule, the procedure of checking contacts, limits the set of generated configurations by exclusion of the unphysical configurations (Fig. 4).

As we have stated above, the purpose of the algorithm was to generate as much different CO_2 locations as possible, which have been subsequently optimized with respect to relative orientation of the host and guest.

All geometry optimizations have been performed with SIESTA implementation of DFT method on the Generalized Gradient Aproximation level, using Perdew–Burke–Erzenhof (PBE) functional,

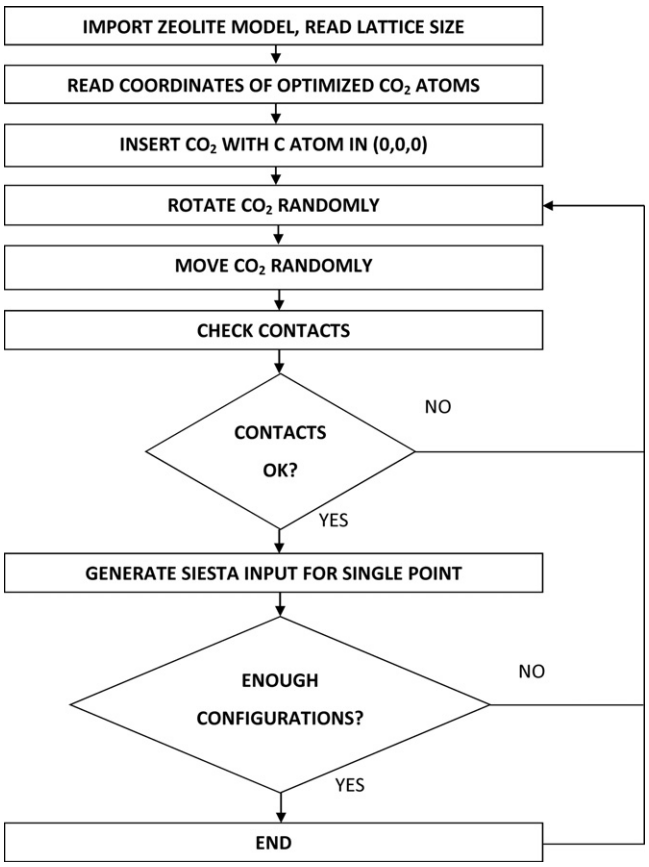

Fig. 3. Block diagram of simple docking algorithm implemented in Zeobuilder.

which was proven to provide good results in this type of calculations [35,36] and DZP basis set. Mesh cutoff was set to 300 Ry and energy tolerance to 0.0001.

The dispersion interactions are important in adsorption of carbon dioxide in zeolites, and one way of implementing it is the dispersion corrections added to the PBE functional [37–39]. In our study, however, the aim was to investigate the influence of the cationic sites, where total interaction is the combination of two types of interactions: CO_2–cation and CO_2–zeolite. We have assumed the interaction with the zeolite framework is always the same, as the DOH structure never changes in our simulations, and the only change is the type of the cation. As the interaction of the

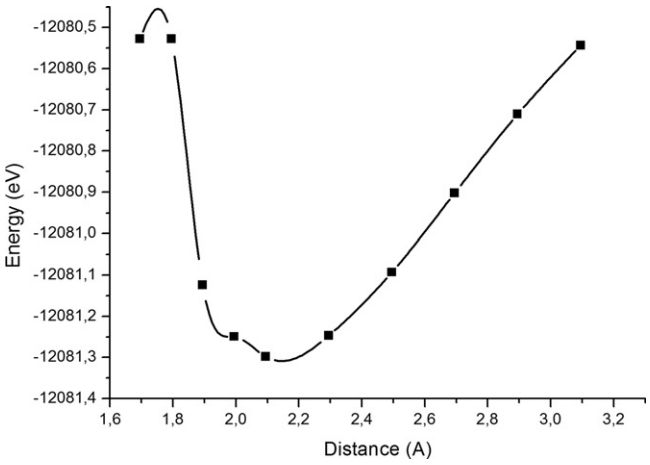

Fig. 4. Total energy (eV) vs. distance.

Table 1
Adsorption energies for structures with Cu, Zn, Ni and Pd cations. Magnitudes lower than E_a for unmodified DOH are in bold. Last column represents CO_2–cation distance. For models with more than one cation, distances to all cations are given, distance to the nearest one is in bold. All units are in eV.

Model	Cu	Zn	Ni	Pd	CO_2–cation distance (Å)]
DOH_4rs_1M	−0.68	−0.72	−0.87	−0.69	5.2
DOH_5rb_1M	−0.96	−1.21	−0.87	−0.79	3.3
DOH_5rs_1M	−0.81	−0.79	−0.86	−0.85	6.8
DOH_6rb_1M	−0.82	−0.85	−0.82	−0.83	6.2
DOH_6rs_1M	−0.64	−0.64	−0.20	−0.72	5.7
DOH_5rb_1M_5rb_1M	−1.18	−1.49	−0.97	−0.88	3.4/3.6
DOH_5rb_1M_5rs_1M_6rs_1M	−0.96	−1.06	−0.94	−0.79	3.1/4.8/6.2
Unmodified DOH	−0.69				

cation is mainly of the electrostatic nature, DFT + D should not play any significant role.

In order to prove that we have carried out the simulations on DFT + D level (as implemented in SIESTA) on a representative model, and found that the interaction is indeed stronger by 0.3 eV with the D2 corrections. However it is independent on the cation present in the system, and the relative energy values would be all corrected by the same value, and therefore the D2 correction can be neglected.

2.3. Molecular dynamics

Molecular Dynamics calculations were carried out using the same SIESTA software with the same PBE functional, the NVT ensemble and Nosé thermostat. Temperature was set to 373 K and time step length 0.5 fs, what allowed us to simulate 10 ps of system's lifetime upon performing 20,000 steps. This lifetime does not allow to study as rare event as the reaction, but allows the system to settle in one of the energetic wells, which cannot be guaranteed by the random nature of the algorithm.

3. Results/discussion

3.1. One adsorption site, several substitution sites

The CO_2 molecule has been introduced into one arbitrarily chosen adsorption site located in the center of the t-doh cage (shown as a gray cage in Fig. 1.). The t-doh site has been chosen, due to its largest dimensions.

Adsorption energies were calculated for structures with Cu^{2+}, Zn^{2+}, Ni^{2+} and Pd^{2+} cations. Results are presented in Table 1. Each row presents results for the same substitution place but for different extra-framework cation.Adsorption energies reach values comparable to adsorption energies calculated on various materials like metal oxides [40], nanotubes [35], γ-Al_2O_3 dopped with transition metals [36]. The experimental value of the adsorption energy of CO_2 on pure MFI zeolite is 0.27 eV [39,40]. There are a few factors that can be the cause of the overestimated value of E_a on DOH vs. MFI. First of all, the different framework structure of MFI with relatively large pores as compared to DOH structure is leading to the better fit of the CO_2 molecule in the DOH tiles than in the MFI channels. Secondly, in our method we investigate E_a in most preferable adsorption sites, while experimental E_a corresponds to the average value of E_a in all occupied adsorption sites, which is equivalent to the GCMC method, which is too computationally demanding on the DFT level at present.

The value of the E_a for unmodified DOH zeolite calculated in this study is −0.69 eV. The presence of cation lowers adsorption energy, intuitively we would expect it only when carbon dioxide molecule is relatively close to the cation (3–3.5 Å). When CO_2 is located far from the cation (5–6 Å), expected adsorption energy change would be very small, even negligible (i.e. less than 0.1 eV, which is the limit for the DFT method as implemented in SIESTA). The results generally confirm this assumptions. The strongest interactions are observed for the model containing 5rb substitutions, as the adsorption site is located in the same cavity and CO_2 molecule can directly interact with the cation.

Copper cations located in 4rs and 6rs substitutions have no influence on the adsorption energy, as they are located further from the adsorption site, and CO_2 interacts only with the silica framework. Situation is the same for Zn and Pd cations, with the strongest interaction of the system with double substitution, and no influence on adsorption energy coming from the cations located farther.

Analysis of the models with 2 cations, leads us to the conclusion that second cation lowers the adsorption energy only when it is located close to CO_2 molecule. This can be explained by the orientation of the CO_2 molecule in the adsorption site. In the model where two oxygen atoms are oriented toward copper cations located just next to the guest molecule, the interaction of one copper cation with the oxygen is doubled with the other cation. Obviously, the cation located in other cage would not interact strongly with CO_2, and therefore only interaction with closely located cation is substantial. This is shown in Fig. 5.

Interestingly, the distance between the cations seems not favorable for the adsorption the CO_2 molecule in between them, as the CO_2 is not located centrally in the middle of the adsorption site. The angles formed by Cu-O-C atoms differ and amount to 132° and 157° respectively (see Fig. 5). We may conclude, that the adsorption site consisting of two cations would be favored in different configuration of Si → Al substitutions or in other zeolite framework.

Another interesting observation is the displacement of the copper cation in the substitution center. The cation located on the left hand side of the Fig. 5 is located in the plane of the 5-ring, but the cation on the right hand side is shifted toward the CO_2 molecule causing distortion of the ring, especially the oxygen bridges.

The model with Ni cation located in 6rs site is the only one in which we can observe the destabilizing effect of the cation, and the E_a amounts only to −0.20 eV.

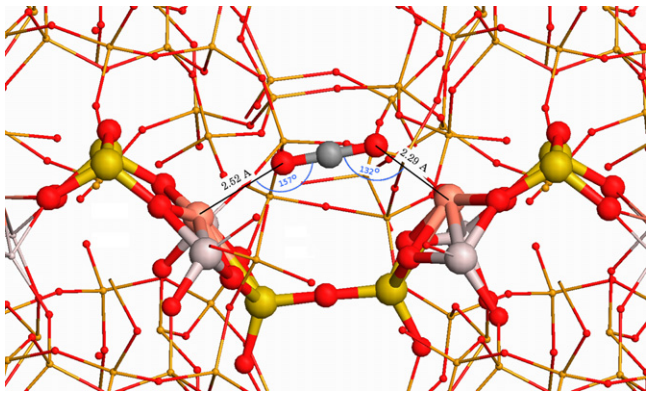

Fig. 5. The orientation of CO_2 in between two cations of the adsorption site.

Table 2
Models with varying location of the CO_2 molecule resulting from docking simulations. Systems with strongest interactions are marked in bold.

Cation	Model	Location	Distance from cation	Adsorption energy
Cu	016	t-red	3.7	−1.29
	023	t-doh	5.6	−0.84
	195	t-red	6.2	−1.26
	226	t-red	6.4	−1.29
	239	t-red	3.7	−1.32
	246	t-red	6.1	−1.27
Ni	003	t-doh	8.5	−0.64
	041	t-doo	3.1	−1.33
	061	t-doh	6.1	−0.95
	068	t-doh	6.7	−0.94
	101	t-red	6.3	−1.18
	151	t-doh	7.4	−0.79
	212	t-red	6.2	−1.33
Zn	014	t-red	3.5	−1.39
	134	t-red	4.0	−1.33
	181	t-doo	2.9	−1.60
	191	t-doh	7.9	−0.78
	242	t-doh	7.0	−0.95
Pd	018	t-doh	6.7	−0.94
	063	t-doo	3.4	−1.23
	079	t-red	6.2	−1.30
	132	t-red	6.2	−1.30

3.2. One substitution site, several adsorption sites

First part of the study allowed us to investigate the interactions of CO_2 located in biggest t-doh cage of the DOH framework, we have no guarantee though that is would be the preferred adsorption site. The CO_2 can fit into smaller t-red and t-doo cages. Our approach for further investigation is based on one model with defined substitution places and cation location. The choice of the model is based on the observation from the above part, that the distance from the substitution plays a crucial role. Therefore it was our intention to promote the substitutions in the smaller cages, as the big ones have been already covered in the first part.

The other option is to choose the multiply substituted model, but this approach would give inconclusive results, as other substitution places can influence the adsorption at the investigated site.

Therefore, we have focused on the 5rs substitution, as it is located in the silicate ring connecting tdoo and tred cages, as we expect it can increase the chance of adsorbing the CO_2 molecule in one of the smaller cages.

As a result of the simulations we have obtained 6 models of the Cu, 7 of Ni, 5 of Zn and 4 of Pd containing systems. They are gathered in Table 2.

The results obtained with the docking tool are consistent with those obtained from the previous part with respect to the guest molecules located in the t-doh tile. The adsorption energies (t-doh) vary from approximately −0.8 eV to −0.9 eV for different cations and CO_2 positions, and most importantly, the order of interaction strength follows the same pattern with different cations.

Intuitively we could expect further lowering of the adsorption energy when the CO_2 molecule was located in the smaller t-red and t-doo cages, as the cation was located in the 5-membered ring connecting those two cages, and therefore the distance to the cation was smaller.

Indeed, the adsorption energies of the CO_2 molecule located in the t-doo tile amount to −1.3 eV, but interactions do not depend on the distance from the Cu cation. That means that the structure of the DOH framework is responsible for most interactions. This is in agreement with first part of this work, where closely located Cu cation lowered the adsorption energy of CO_2 only by 0.1 eV.

Similarly for the Ni cation, the adsorption of CO_2 is stronger in t-doo cage than in t-doh, and the energy amounts to −1.2 eV to −1.3 eV. The CO_2 molecule adsorbed in the t-red cage result in the strongest adsorption energy, and the effect of tight cage is enhanced by the close presence of Ni cation.

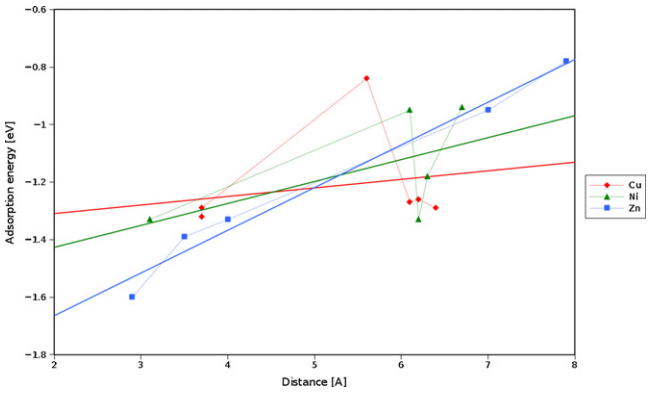

Fig. 6. The correlation between the adsorption energy and the distance of the guest molecule from the cation.

The same holds for Zn, where CO_2 located in t-doh is weakly adsorbed (−0.7 to −0.9 eV), and in tdoo the adsorption is significantly stronger (approximately −1.3 eV). The strongest adsorption has been observed for the CO_2 located in tred cage of the DOH zeolite containing Zn and amounted to −1.6 eV.

Only the model containing a Pd cation gives opposite results—the CO_2 molecule adsorbed in t-red cage is bound weaker than in t-doo despite the closer distance to the cation. This might be the result of the distortion of the DOH framework caused by large Pd cation. This observation is also consistent with MD simulations presented further in Section 3.3.

The distance–adsorption energy relationship can be confirmed by the correlation analysis, shown in Fig. 6. Although the number of data points is too small for accurate analysis, it is clearly seen, that there are two groups of points on the plot—first represents the CO_2 molecule adsorbed in the same tile as the cation is present, while the other group represents the adsorption in neighboring tile, where the distances from the cation are greater than 5 Å. The trend lines have all positive coefficients, what means that the energies increase with the distance.

The Zn trend line deserves particular attention, as the correlation between the energies and the distance is very good. We conclude, that this is due to the strength of interaction with the Zn cation, which (partially) overshadows the interaction between the CO_2 molecule and the DOH framework, especially in the range up to 4 Å. As the interactions of CO_2 with other cations are weaker, the correlation suffers from the effect of the interaction with the framework.

3.3. Molecular dynamics

For further analysis we have chosen 4 models containing Cu, Ni, Pd and Zn. For each of these models we have carried out a molecular dynamics simulation lasting for 10 ps.

During MD simulation of model with Zn cation, carbon dioxide molecule is asymmetric (one of the C—O bonds is longer than the other) (see Fig. 7). The asymmetry is not strong though the average differences in the bond lengths reach the values not greater than 0.04 Å. This effect, but slightly less intensive, is visible for models with Cu (only that one, where CO_2 is close to the cation) and Ni. Dynamics for Pd model leads to different results—no CO_2 asymmetry can be observed, as it is for model where Cu is located far from cation.

This can be explained by weak interactions between the CO_2 molecule and the cation, however the sources of these weak

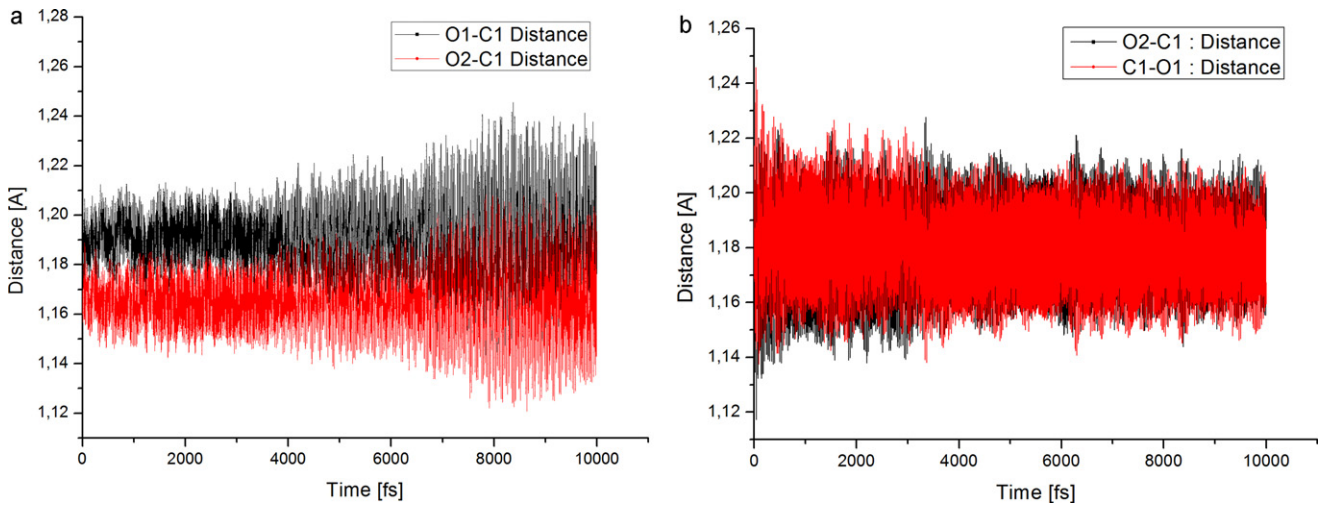

Fig. 7. Changes in the C—O bond lengths in time for model with Zn cation (a) and Pd cation (b).

interactions are different. Whereas for the Pd case, the reason is a combination of electron configuration, size of the cation and distortion of the zeolite framework structure, in case of Cu it clearly is the further distance from the adsorption site which makes the electrostatic screening possible.

Distance between Zn cation and O atom from CO_2 molecule oscillate around 2.2 Å (what is the exact value of the arithmetic mean) (see Fig. 7a). This value is only a little greater than Zn–O distance in Wurtzite (1.98 Å) and in zinc blende (2.00 Å) [25]. That means, that the strength of interaction between Zn cation and O from CO_2 molecule is comparable to the strength of ionic bond in the ZnO crystal. Interestingly, the vibrations of the C and O_2 atom show similar pattern, while the O1 atom's motion is not consistent with C and O_2. This observation confirms strong interaction between Zn cation and O atom, observed already in previous sections. Interaction with Zn is strong enough to "lock" oxygen atom in the place close to the cation, so it vibrates independently from C and O_2. Moreover, the oscillations of O1 are least intensive from all of the investigated models. This allows us to conclude that the system should rather be treated ad CO molecule adsorbed to ZnO center (Fig. 8).

Cu model (with CO_2 molecule located close to the cation) leads to results similar to Zn, however the oscillations are more intensive than in case of Zn, and the "locking" of one O atom cannot be observed.

Opposite behavior of CO_2 is observed in Pd model, where weak Pd–O interaction allows molecule to move further, rotate and change the orientation in 3 ps time. All oscillations are consistent what clearly indicates the motion of whole molecule, and not independent parts of it (see Fig. 7b). The same holds for Cu model, where molecule is located far from the cation.

Similarly to the Pd model, carbon dioxide molecule in model with Ni cation, changes its orientation with respect to the cation and is placed sideways. However, after a short time, CO_2 returns to initial orientation (with one of the oxygens directed toward the cation) and holds in this position to the end of simulation. The effect comes together with the change of the CO_2 bonds lengths—the molecule becomes symmetric during the time of lateral orientation of CO_2 with respect to the cation, while it is asymmetric during the rest of simulation.

Changes of O—C—O angle in Ni model may indicate the activation of the CO_2 molecule, as the value of the angle decreases to 167° at ~8 ps of the run, but neither distances nor energies confirm that, and therefore we conclude it is only due to the thermal motions of CO_2. On the other hand, for Zn model, the decrease of the angle (at approximately 5 ps) corresponds to the change in oscillations of C—O bonds (Fig. 9) (see Figs. 6a and 7b).

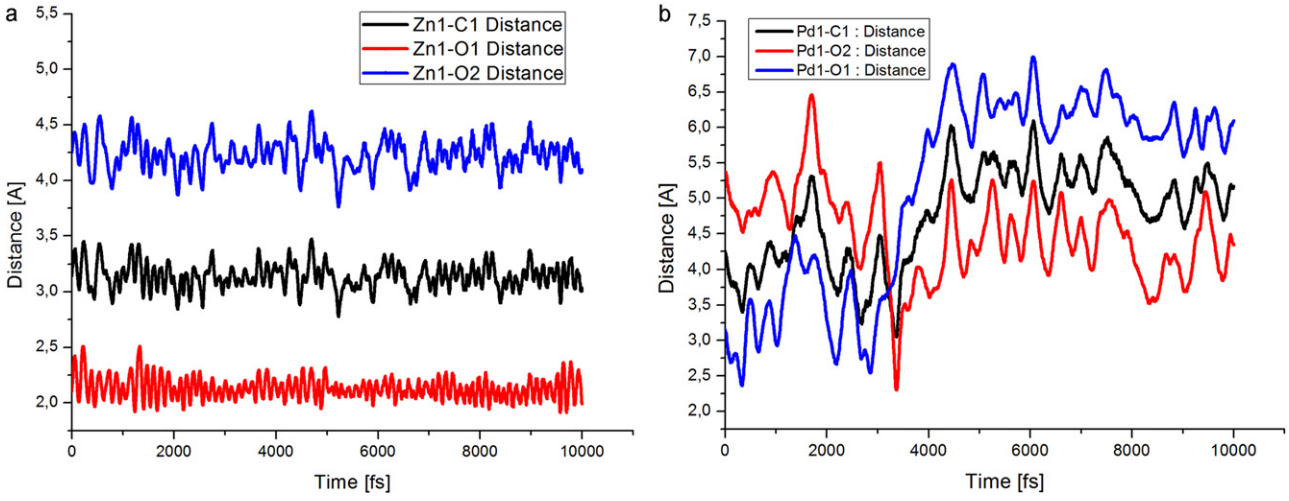

Fig. 8. Distances between Zn cation (a), Pd cation (b) and CO_2 molecule during the MD run.

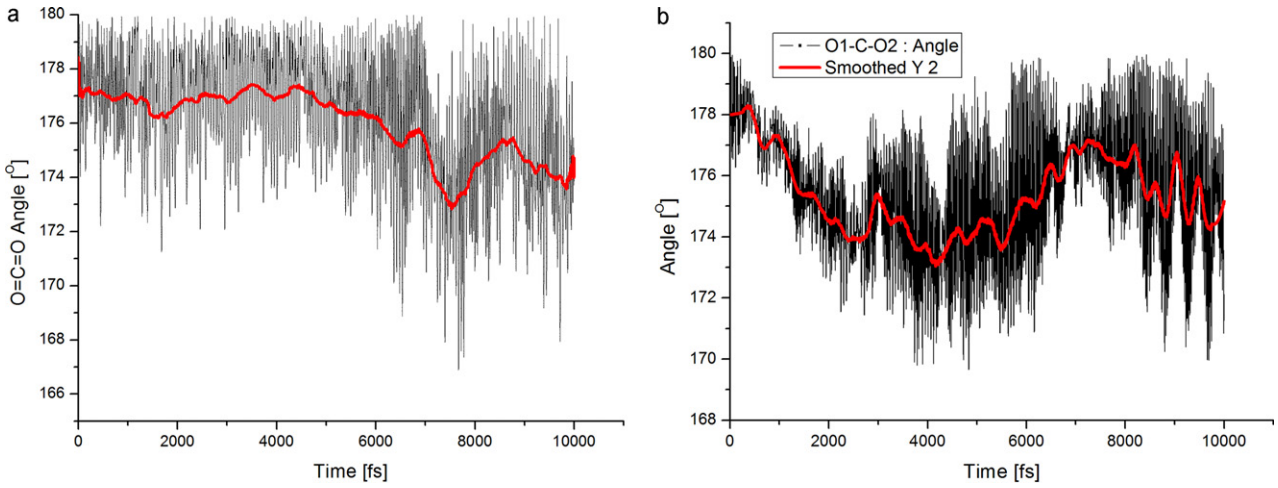

Fig. 9. Changes in O—C—O angle during the MD run for model with Ni cation (a) and Zn cation (b).

4. Conclusions

Seeking the most favorable adsorption site is a non-trivial problem. For studied systems, different cages present in the zeolite cause different local minima of the energy, what effectively makes finding the global minimum difficult. Docking tool developed for the purpose of this study and presented in this paper seems to be promising solution to this issue, although the algorithm needs some improvements, especially in the term of accepting/rejecting configurations.

Different approaches for simulations performed for the needs of this work, allowed us to find the influence of the type of a cation in the zeolite structure on carbon dioxide adsorption. Additionally, the shorter the distance between CO_2 and cation, the lower the adsorption energy is, which together with the changes in the oscillations and the asymmetry of the CO_2 molecule makes the cation not only the adsorption center but also potential catalytic site.

Molecular dynamics simulations allowed us to find, that CO_2, while close to Zn cation, gets "locked" in one position—rotation or translation is impossible, whereas carbon dioxide molecule far from cation has some translation freedom and full rotation freedom. The asymmetry mentioned above has also been confirmed to be dependent on the distance from the cation.

Acknowledgements

The work was financed by a statutory activity subsidy from the Polish Ministry of Science and Higher Education for the Faculty of Chemistry of Wrocław University of Technology. Calculations were carried out using computational resources of Wroclaw Center of Networking and Supercomputing and Interdisciplinary Centre for Mathematical and Computational Modelling.

References

[1] Q. Wang, J. Luo, Z. Zhong, A. Borgna, CO_2 capture by solid adsorbents and their applications: current status and new trends, Energy & Environmental Science 4 (2011) 42–55.
[2] M.R. Raupach, G. Marland, P. Ciais, C. Le Quere, J.G. Canadell, G. Klepper, C.B. Field, Global and regional drivers of accelerating CO_2 emissions, Proceedings of the National Academy of Science 104 (2007) 10288–10293.
[3] T. Conway, P. Tans, NOAA/ESRL, (www.esrl.noaa.gov/gmd/ccgg/trends/) (September 2011).
[4] K.M.K. Yu, I. Curcic, J. Gabriel, S.C.E. Tsang, Recent advances in CO_2 capture and utilization, ChemSusChem 1 (2008) 893–899.
[5] M.V. Sivaiaha, B.S. Petit, B.J. Barrault, C. Batiot-Dupeyrat, S. Valange, CO_2 reforming of CH_4 over Ni-containing phyllosilicates as catalyst precursors, Catalysis Today 157 (2010) 397–403.
[6] M.R. Gonçalves, A. Gomes, J. Condeço, R. Fernandes, T. Pardal, C.A.C. Sequeira, J.B. Branco, Selective electrochemical conversion of CO_2 to C_2 hydrocarbons, Energy Conversion and Management 51 (2010) 30–32.
[7] E.I. Papaioannou, S. Souentie, A. Hammad, C.G. Vayenas, Electrochemical promotion of the CO_2 hydrogenation reaction using thin Rh, Pt and Cu films in a monolithic reactor at atmospheric pressure, Catalysis Today 146 (2009) 336–344.
[8] J. Ma, N. Sun, X. Zhang, N. Zhao, F. Xiao, W. Wei, Y. Sun, A short review of catalysis for CO_2 conversion, Catalysis Today 148 (2009) 221–231.
[9] S. Wang, D. Mao, X. Guo, G. Wu, G. Lu, Dimethyl ether synthesis via CO_2 hydrogenation over CuO–TiO_2–ZrO_2/HZSM-5 bifunctional catalysts, Catalysis Communications 10 (2009) 1367–1370.
[10] W. Wang, S. Wang, X. Ma, J. Gong, Recent advances in catalytic hydrogenation of carbon dioxide, Chemical Society Reviews 40 (2011) 3703–3727.
[11] D. Luo, N. Zhang, S. Hong, H. Wu, Z. Liu, Complexes in the photocatalytic reaction of CO_2 and H_2O: theoretical studies, International Journal of Molecular Sciences 11 (2010) 2792–2804.
[12] Y. Li, W. Wang, Z. Zhan, M. Woo, C. Wu, P. Biswas, Photocatalytic reduction of CO_2 with H_2O on mesoporous silica supported Cu/TiO_2 catalysts, Applied Catalysis B 100 (2010) 386–392.
[13] R.W. Dorner, D.R. Hardy, F.W. Williams, H.D. Willauer, Heterogeneous catalytic CO_2 conversion to value-added hydrocarbons, Energy & Environmental Science 3 (2010) 884–890.
[14] R.B. Anderson, Thermodynamics of the hydrogenation of oxides of carbon, Journal of Physical Chemistry 90 (1986) 4806–4810.
[15] V.P. Indrakanti, H.H. Schobert, J.D. Kubicki, Quantum mechanical modeling of CO_2 interactions with irradiated stoichiometric and oxygen-deficient anatase TiO_2 surfaces: implications for the photocatalytic reduction of CO_2, Energy and Fuels 23 (2009) 5247–5256.
[16] A.M. Khenkin, I. Efremenko, L. Weiner, J.M.L. Martin, R. Neumann, Photochemical reduction of carbon dioxide catalyzed by a ruthenium-substituted polyoxometalate, Chemistry – A European Journal 16 (2010) 1356–1364.
[17] K.-W. Huang, J.H. Han, C.B. Musgrave, E. Fujita, Carbon dioxide reduction by pincer rhodium η2-dihydrogen complexes: hydrogen-binding modes and mechanistic studies by density functional theory calculations, Organometallics 26 (2007) 508–513.
[18] R.W. Dorner, D.R. Hardy, F.W. Williams, H.D. Willauer, Effects of ceria-doping on a CO_2 hydrogenation iron–manganese catalyst, Catalysis Communications 11 (2010) 816–819.
[19] W.C. Chueh, C. Falter, M. Abbott, D. Scipio, P. Furler, S.M. Haile, A. Steinfeld, High-flux solar-driven thermochemical dissociation of CO_2 and H_2O using nonstoichiometric ceria, Science 330 (2010) 1797–1801.
[20] M.S.G. Ahlquist, Iridium catalyzed hydrogenation of CO_2 under basic conditions—mechanistic insight from theory, Journal of Molecular Catalysis A: Chemical 324 (2010) 3–8.
[21] H. Yamashita, K. Ikeue, T. Takewaki, M. Anpo, In situ XAFS studies on the effects of the hydrophobic–hydrophilic properties of Ti-beta zeolites in the photocatalytic reduction of CO_2 with H_2O, Topics in Catalysis 18 (2002) 95–100.
[22] M. Anpo, H. Yamashita, K. Ikeue, Y. Fujii, S.G. Zhang, Y. Ichihashi, D.R. Park, Y. Suzuki, K. Koyano, T. Tatsumi, Photocatalytic reduction of CO_2 with H_2O on Ti-MCM-41 and Ti-MCM-48 mesoporous zeolite catalysts, Catalysis Today 44 (1998) 327–332.
[23] M. Anpo, H. Yamashita, Y. Ichihashi, Y. Fujii, M. Honda, Photocatalytic reduction of CO_2 with H_2O on titanium oxides anchored within micropores of zeolites: effects of the structure of the active sites and the addition of Pt, Journal of Physical Chemistry B 101 (1997) 2632–2636.
[24] B. Liu, B. Smit, Langmuir 25 (10) (2009) 5918–5926.
[25] Materials Studio (Accelrys Inc.) database of structures, http://accelrys.com/products/materials-studio (September 2011).

[26] Database of Zeolite Structures, Framework Type DOH http://izasc.ethz.ch/fmi/xsl/IZA-SC/ftc_fw.xsl?-db=Atlas_main&-lay=fw&-max=25&STC=DOH&-find (September 2012).
[27] J.T. Miller, E. Glusker, R. Peddi, T. Zheng, J.R. Regalbuto, The role of acid sites in cobalt zeolite catalysts for selective catalytic reduction of NO_x, Catalysis Letters 51 (1998) 15–22.
[28] E.A. Pidko, P. Mignon, P. Geerlings, R.A. Schoonheydt, R.A. van Santen, A periodic DFT study of N_2O_4 disproportionation on alkali-exchanged zeolites X, Journal of Physical Chemistry C 112 (2008) 5510–5519.
[29] I.L.C. Buurmans, E.A. Pidko, J.M. de Groot, E. Stavitski, R.A. van Santen, B.M. Weckhuysen, Styrene oligomerization as a molecular probe reaction for zeolite acidity: a UV–vis spectroscopy and DFT study, Physical Chemistry Chemical Physics 12 (2010) 7032–7040.
[30] T. Verstraelen, V. Van Speybroeck, M. Waroquier, ZEOBUILDER. A GUI toolkit for the construction of complex molecular structures on the nanoscale with building blocks, Journal of Chemical Information and Modeling 48 (2008) 1530–1541.
[31] P. Ordejón, E. Artacho, J.M. Soler, Selfconsistent order-N density-functional calculations for very large systems, Physical Review B: Rapid Communications 53 (1996) R10441–R10443.
[32] J.M. Soler, E. Artacho, J.D. Gale, A. García, J. Junquera, P. Ordejón, D. Sánchez-Portal, The SIESTA method for ab initio order-N materials simulation, Journal of Physics: Condensed Matter 14 (2002) 2745–2779.
[33] D. Frenkel, B. Smit, Chapter 3—Monte Carlo simulations, in: Understanding Molecular Simulation, 2nd ed., Academic Press, 2002, 23–61.
[34] R.A. van Santen, Theory of bronsted acidity in zeolites, Studies in Surface Science and Catalysis 85 (1994) 273–294.
[35] J. Zhao, Y. Ding, Can silicon carbide nanotubes sense carbon dioxide, Journal of Chemical Theory and Computation 5 (2009) 1099–1105.
[36] Y. Pan, C. Liu, T.S. Wiltowski, Q. Ge, CO_2 adsorption and activation over γ-Al_2O_3-supported transition metal dimers: a density functional study, Catalysis Today 147 (2009) 68–76.
[37] S. Grimme, Semiempirical GGA-type density functional constructed with a long-range dispersion correction, Journal of Computational Chemistry 27 (2006) 1787–1799.
[38] S. Grimme, J. Antony, S. Ehrlich, H. Krieg, A consistent and accurate ab initio parametrization of density functional dispersion correction (DFT-D) for the 94 elements H Pu, Journal of Chemical Physics 132 (154104) (2010) 1–19.
[39] A. Pulido, M.R. Delgado, O. Bludsky, M. Rubes, P. Nachtigall, C.O. Arean, Combined DFT/CC IR spectroscopic studies on carbon dioxide adsorption on the zeolite H-FER, Energy & Environmental Science 2 (2009) 1187–1195.
[40] R. Hammami, A. Dhoui, S. Fernandez, C. Minot, CO_2 adsorption on (0 0 1) surfaces of metal monoxides with rock-salt structure, Catalysis Today 139 (2008) 227–233.